Phys. Status Solidi C **9**, No. 3–4, 572–575 (2012) / **DOI** 10.1002/pssc.201100442

Improved crystalline quality and light output power of GaN-based light-emitting diodes grown on Si substrate by buffer optimization

Xinbo Zou, Ka Ming Wong, Naisen Yu, Peng Chen, and Kei May Lau*

Department of Electronic and Computer Engineering, Hong Kong University of Science & Technology, Clear Water Bay, Kowloon, Hong Kong

Received 10 July 2011, revised 7 September 2011, accepted 21 November 2011
Published online 30 January 2012

Keywords GaN on Si, LED, flow modulation, superlattice

* Corresponding author: e-mail eekmlau@ust.hk, Phone: +852 2358 7049, Fax: +852 2358 1485

High-quality crack-free GaN-based light-emitting diodes (LEDs) were grown on patterned Si substrate using a flow modulation method and a high-temperature (HT)-AlN/AlGaN superlattice structure (SLs) interlayer. The effects of these two techniques on material properties and device performance were studied. The enhanced crystalline quality can be attributed to a 3D to 2D coalescence process with fewer dislocations initiated from the interlayers. The light output power of blue LEDs was improved by 66% after successful implementation of flow modulation and new interlayers. After substrate removal and packaging, the optical power of circle LEDs with diameter of 300 μm could reach as high as 6.30 mW at 20 mA.

© 2012 WILEY-VCH Verlag GmbH & Co. KGaA, Weinheim

1 Introduction

GaN grown on silicon (111) have been widely investigated because of silicon's advantages such as low manufacturing cost, large size availability, and good thermal conductivity [1-4]. However, large mismatch in lattice constant would cause a large amount of defects in the order of 10^{10} cm^{-2} during hetero-epitaxy. And cracks easily develop in the high temperature process especially when the GaN layer thickness exceeds 1 μm because of huge thermal coefficient mismatch between GaN and Si.

Many techniques have been reported for defect reduction and crack elimination. SiN_x interlayer, which is inserted at different positions by different groups, [2, 4, 5] has been proved to be an effective method to suppress dislocations.

AlN-based buffer is also widely used to provide compressive stress for strain balancing as AlN has a smaller lattice constant than GaN (2%) [6]. Dual-AlN interlayers [4], and step-graded $Al_xGa_{1-x}N$ buffer layer [7] between AlN nucleation layer and GaN have been reported to achieve crack-free GaN.

There are many publications reporting GaN growth on silicon substrates, but few included results of LED devices. In this paper, we present improved GaN crystalline quality and GaN-based LED performance after effective implementation of a flow modulation method and a HT-AlN/AlGaN SLs interlayer. Detailed LED results including those after Si substrate removal and packaging are also reported.

2 Experimental

The growth of GaN films were performed on patterned-silicon substrates by MOCVD in an Aixtron 2000HT system. Detailed Si substrate preparations can be found elsewhere [2]. Trimethylgallium (TMGa), trimethylaluminum (TMAl), and ammonia (NH_3) were used as precursors for Ga, Al, and N, respectively. To compare the crystalline quality of GaN grown by different methods, three samples A, B and C were grown with the same film thickness. The growth details were as follows:

Firstly, a 30 nm AlN nucleation layer and an in-situ SiN_x mask were deposited on the silicon substrate. Secondly, 1 μm GaN was then grown using a fixed [NH_3]/[TMGa] molar ratio of 900 for Sample A, or flow modulation method, with a step-increase of [NH_3]/[TMGa] ratio from 390 to 900 and then 1600, for Sample B and C. Thirdly, Sample A and B shared the same low-temperature (LT)-

© 2012 WILEY-VCH Verlag GmbH & Co. KGaA, Weinheim

AlN/HT-AlGaN as interlayer, while Sample C adopted 8 pairs of HT-AlN/AlGaN SLs as interlayer. Finally, 1.5 µm intrinsic GaN (i-GaN) was grown on top for all three samples. The growth details are summarized in Table 1.

Furthermore, four LED wafers were prepared to investigate LED performance with different buffers. LED wafers (LA, LB and LC1) were grown with buffers similar to Sample A, B and C, respectively. Each LED structure consists of a 1.5-µm Si-doped n-GaN layer, 5 periods of InGaN/GaN MQWs and a 200-nm-thick Mg-doped p-GaN layer. LED wafer LC2 adopted the same growth method as LC1 but with an extended n-GaN thickness to 2 µm.

Table 1 Growth details of three samples. LT and HT denote reactor temperature of 950 °C and 1130 °C, respectively.

Sample	GaN buffer growth	Interlayer composition
A	$[NH_3]/[TMGa] = 900$	10 nm LT-AlN /250 nm HT-AlGaN
B	Flow modulation method	
C		SLs: 8 × 5 nm HT-AlN /25 nm HT-AlGaN

3 Results and discussion

3.1 Material characterization

Crystalline quality of all three samples A, B and C was examined by high-resolution X-ray diffraction (HRXRD), as shown in Fig. 1. The effects of the flow modulation were investigated by comparing Sample A with Sample B. The full-width at half-maximum (FWHM) of Sample B was narrowed for both (002) and (102) orientation compared with Sample A, which can be attributed to enhanced three-dimensional (3D) growth during the initial stage of the i-GaN layer. As shown in Fig. 2(b), when a low $[NH_3]/[TMGa]$ ratio was adopted, the reflectivity dropped quickly to nearly zero and no interference was observed. Under this condition, lateral growth was suppressed and large GaN island size formed [8] leading to smaller density of islands and a rough surface. Afterwards, by increasing $[NH_3]/[TMGa]$ molar ratio, lateral growth was accelerated and those large GaN islands started to coalescence. The reflectivity of Sample B increased gradually and many dislocation lines got bent and terminated, leading to a better quality of the GaN epilayer. While in Fig. 2(a), a clear interference in the beginning of GaN growth can be observed, showing a smoother surface than that in Sample B. In the subsequent growth of GaN, the dislocation lines had less chance to get bent compared with Sample B, and would propagate along the growth direction.

Compared with Sample B, the FWHM of Sample C was even narrower, together with higher peak intensity, which indicated its superior quality over Sample B after introduction of SLs as interlayer. The effects of HT-AlN/AlGaN SLs interlayer can be understood by comparing cross-sectional TEM photos of Sample B and C, as shown in Fig. 3. The bright field images were collected near the GaN [1-100] zone axis under multi-beam diffraction conditions so that all types of threading dislocations can be visible. It is observed that a large amount of dislocations initiated from the LT-AlN layer and can be found in the subsequent HT-AlGaN and GaN layers. While in Sample C, the TD density inside and above the interlayer was much smaller than that of Sample B. The dislocation density of top GaN layer in Sample B and Sample C were 6.6×10^9 cm^{-2} and 5.0×10^9 cm^{-2}, derived from Fig. 3.The better crystalline quality of Sample C as indicated by its narrower FWHM of XRD rocking curves can be correlated to its reduced TD density generated in the interlayer.

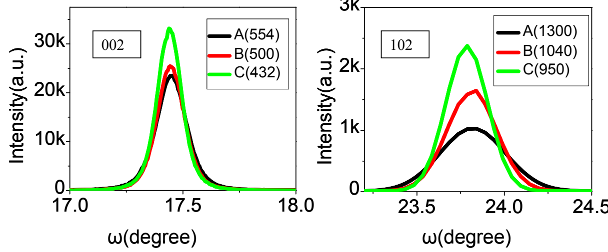

Figure 1 Symmetric (002) and asymmetric (102) HRXRD rocking curves of Sample A, B and C. Corresponding FWHMs were listed in brackets in the unit of arcsec.

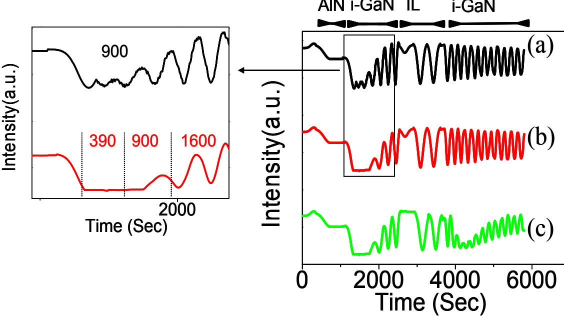

Figure 2 In-situ reflectance spectra of GaN growth on silicon of Sample A (a), B (b) and C (c). The numbers indicated the $[NH_3]/[TMGa]$ molar ratio in different time-slots for Sample A and B. IL denotes interlayer.

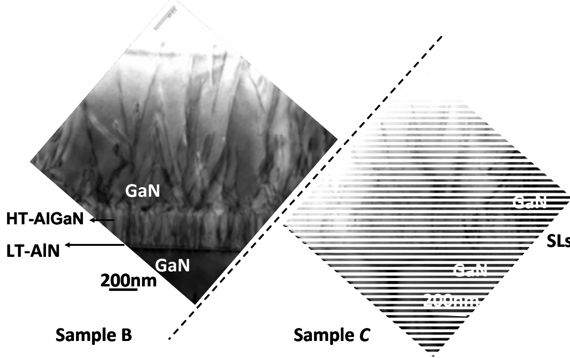

Figure 3 Cross-sectional TEM images of Sample B and C.

© 2012 WILEY-VCH Verlag GmbH & Co. KGaA, Weinheim

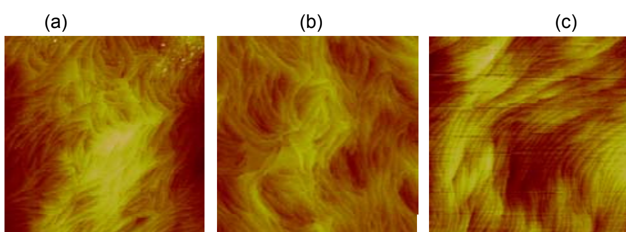

Figure 4 AFM images (5 μm × 5 μm scans) of GaN films in Sample A (a), Sample B (b), Sample C (c).

The surface morphology of each sample was investigated by atomic force microscopy (AFM), as shown in Fig. 4. All three samples exhibited very smooth surface and clear atomic steps with root-mean-square (RMS) roughness at 0.7 nm level. Among the three pictures, the atomic steps of Sample C are the best aligned with a distance between the steps of about 180 nm, which also confirmed its best crystalline quality among the three.

Micro-Raman was also employed to investigate the stress states. The stress-sensitive E_2 (high) phonon band positions were collected and slightly corrected with intense Si phonon reference band at 520.2 cm^{-1}, as shown in Fig. 5. With respect to stress-free homoepitaxially grown GaN band at 567.5 cm^{-1}, Sample A suffered the largest tensile stress, as estimated to be 1.08 GPa [9]. While the introduction of flow modulation in Sample B, and added HT-AlN/AlGaN SLs interlayer into Sample C, residual tensile stress was gradually released to be 0.81 GPa and 0.44 GPa, respectively.

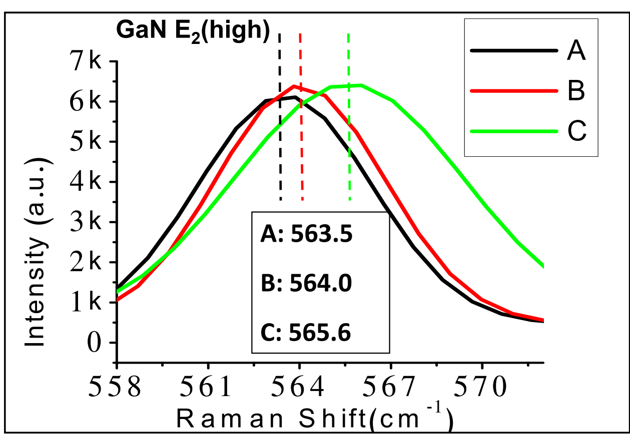

Figure 5 Raman Spectrum of E_2 (high) phonon bands for Sample A, B and C.

3.2 LED results

Photoluminescence (PL) of four LED wafers was measured using a 325 nm He-Cd laser as the excitation source, as shown in Fig. 6(a). The PL peak intensity can be divided into three levels: LA is the weakest while LC2, whose FWHMs of XRD ω-scans for the (002) and (102) orientation were 426 arcsec and 910 arcsec, emitted the most light. The remaining two samples, LB and LC1, shared a similar medium amount of emitted light.

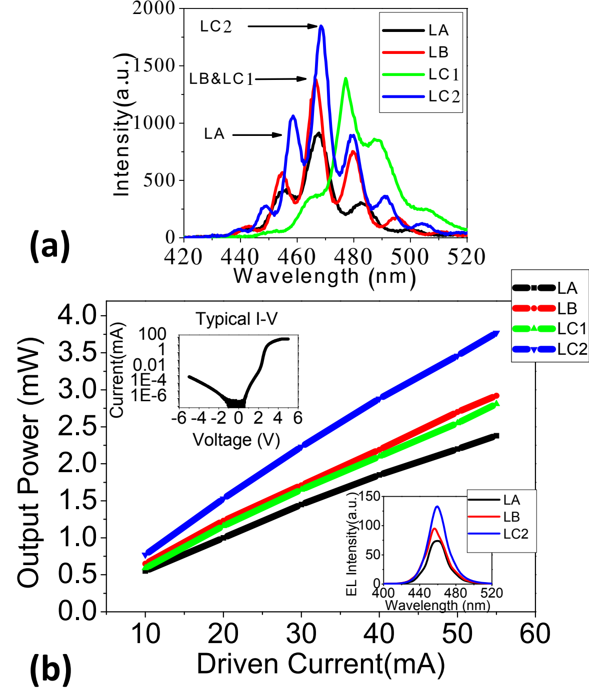

Figure 6 PL spectrums of four LED wafers at room temperature (a) and L-I characterizations of four LEDs on Si (b). A typical I-V curve was shown inset (left-top) and EL spectrums of 500 μm × 500 μm square LEDs LA, LB and LC2 driven at 55 mA were shown also (right-bottom).

LEDs were fabricated with all four wafers using a standard three-mask process. Figure 6(b) shows the light output power versus injection current (L-I) characteristics of 500 μm × 500 μm square LEDs with different buffers after the standard fabrication process. The output power of each LED was quite linear to the driven current. The current-voltage (I-V) characteristics were similar to each other for all LEDs and a typical I-V curve was plotted in the top-left inset of Fig. 6(b). Typically, the forward voltage of a 500 μm × 500 μm square LED was (3.4 ± 0.1) V driven at 20 mA, and (4.0 ± 0.1) V at 55 mA. And the leakage current at reverse-bias of -5 V was (0.7 ± 0.1) μA. When the same 55 mA current was applied, 2.00 mW blue light was measured from LA, while LEDs LB, LC1 and LC2 emitted 2.60 mW, 2.56 mW and 3.33 mW, respectively, corresponding to 30%, 28% and 66% improvement in power. The electroluminescence (EL) spectrums of LA, LB and LC2 driven at 55 mA were shown in the bottom-right inset of Fig. 6(b). The EL performance agrees with the PL measurements well and it can also be concluded that internal quantum efficiency was enhanced as the GaN quality was improved and GaN thickness was increased. It's noted that the optical power of LC1 almost levelled with that of LB in both PL and EL measurements with longer wavelength of around 10 nm, although the growth conditions of LC1 gave better crystalline quality. This maybe due to stronger quantum-confined Stark effect (QCSE) in quan-

© 2012 WILEY-VCH Verlag GmbH & Co. KGaA, Weinheim

tum wells impacted by SLs interlayer [10]. Thus, the benefit of improved crystalline quality was compensated by QCSE under 1.5 μm n-GaN condition.

Beyond the standard process, the silicon substrate of LC2 was removed and LEDs were transferred onto a copper substrate [11]. Furthermore, LEDs LC2 on copper were simply packaged by hemisphere silicone dome to reduce total internal reflection. The light output power of two different-sized LC2 at different stages were measured and listed in Table 2.

Table 2 Light output power of different-sized LC2 at different process stages. The diameter of the circular LEDs is 300 μm and the edge of square LEDs is 500 μm long.

Light output power (mW)	Circular LED @20 mA	Square LED @55 mA
On silicon	1.29	3.33
On copper	2.35	5.85
After package	6.30	14.00

4 Conclusion

In summary, GaN epilayers were optimized by introducing flow modulation method and a HT-AlN/AlGaN SLs interlayer. Crystalline quality, surface mophorlogy and residual tensile stress were significantly improved after optimization. Crack-free GaN-based LEDs with total thickness of 3.3 μm were demostrated using optimized growth methods and structure. Optical power was measured to be 3.33 mW from 500 μm × 500 μm LEDs at 55 mA while on the original growth substrate, giving a power improvement of 66% compared with that before optimizaiton. After Si removal and simple packaging, the light output power could reach 5.85 mW and 14.00 mW, respectively under the same measurement conditions.

Acknowledgements This work was supported in part by the Research Grants Council under Grant 615705 and in part by the Innovation and Technology Commission of the Hong Kong Special Administrative Government under Grant GHP/034/07GD.

References

[1] A. Krost and A. Dadgar, Mater. Sci. Eng. B **93**(1-3), 77 (2002).

[2] B. Zhang, H. Liang, Y. Wang, Z. Feng, K. Ng, and K. M. Lau, J. Cryst. Growth **298**, 725 (2007).

[3] D. Deng, N. Yu, Y. Wang, X. Zou, H.-C. Kuo, P. Chen, and K. M. Lau, Appl. Phys. Lett. **96**(20), 201106 (2010).

[4] A. Dadgar, M. Poschenrieder, J. Bläsing, O. Contreras, F. Bertram, T. Riemann, A. Reiher, M. Kunze, I. Daumiller, A. Krtschil, A. Diez, A. Kaluza, A. Modlich, M. Kamp, J. Christen, F. A. Ponce, E. Kohn, and A. Krost, J. Cryst. Growth **248**, 556 (2003).

[5] E. Arslan, M. K. Ozturk et al., Curr. Appl. Phys. **9**(2), 472-477 (2009).

[6] H. Amano, M. Iwaya, T. Kashima, M. Katsuragawa, I. Akasaki, J. Han, S. Hearne, J. A. Floro, E. Chason, and J. Figiel, Jpn. J. Appl. Phys., Part 2: Letters **37,** L1540 (1998).

[7] K. Cheng, M. Leys et al., Appl. Phys. Lett. **92**(19), 192111 (2008).

[8] T. Yang, K. Uchida et al., Phys. Status Solidi A **180**(1), 45 (2000).

[9] C. Kisielowski, J. Kruger et al., Phys. Rev. B **54**(24), 17745 (1996).

[10] B. A. B. A. Shuhaimi, A. Watanabe, and T. Egawa, Jpn. J. Appl. Phys. **49,** 021002 (2010).

[11] K. M. Wong, X. Zou, P. Chen, and K. M. Lau, IEEE Electron Device Lett. **31**(2), 132 (2010).

© 2012 WILEY-VCH Verlag GmbH & Co. KGaA, Weinheim